JOURNAL OF GEOPHYSICAL RESEARCH, VOL. 105, NO. A10, PAGES 23,153–23,165, OCTOBER 1, 2000

A review on the genesis of coronal mass ejections

T. G. Forbes

Institute for the Study of Earth, Oceans, and Space, University of New Hampshire, Durham

Abstract. This paper provides a short review of some of the basic concepts related to the origin of coronal mass ejections (CMEs). The various ideas which have been put forward to explain the initiation of CMEs are categorized in terms of whether they are force-free or non-force-free and ideal or nonideal. A few representative models of each category are examined to illustrate the principles involved. At the present time there is no model which is sufficiently developed to aid forecasters in their efforts to predict CMEs, but given the current pace of research, this situation could improve dramatically in the near future.

1. Introduction

Figure 1 illustrates three different types of large-scale eruptive phenomena occurring in the solar atmosphere, specifically coronal mass ejections (CMEs), prominence eruptions, and large flares. They are all closely related and may, in fact, be different manifestations of a single physical process. Let us first consider the CME.

Here we will use the term "CME" to indicate the entire process that leads to the ejection of mass and magnetic flux into interplanetary space. Traditionally, observers have defined a CME as the outward traveling bright arc seen in coronagraphs (Figure 1a) and the dark cavity (also Figure 1a), prominence material (Figure 1b), and X-ray loops (Figure 1d) that appear behind this arc are not considered as the CME even though they are associated with it. The bright arc is thought to result from the pileup of the helmet streamer which typically overlies the erupting region [*Hundhausen*, 1988; *Low*, 1996], but most of the models we discuss here do not include a helmet streamer. Since there is no feature in these models which can be associated with the bright arc, they are not models of CMEs according to the standard definition of many observers. However, for a general theoretical discussion we need to have a term which refers not just to an isolated feature seen by a particular instrument but to the underlying physical reality of the entire phenomenon. Already many researchers use the term CME in just this way. Even though this creates a certain degree of confusion, it is natural for the definition of a phenomenon to evolve from one that is based purely on observational aspects to one that is based on an understanding of the physical phenomenon itself.

CMEs constitute large-scale ejections of mass and magnetic flux from the lower corona into the interplanetary medium. Measurements from spacecraft and coronagraphs show that a typical CME injects roughly 10^{23} Maxwells of magnetic flux and 10^{16} g of plasma into interplanetary space [*Gosling*, 1990; *Webb et al.*, 1994]. During the quiet phase of the solar cycle there are approximately two CMEs per week, but during the active phase the rate can exceed one per day. Although most CMEs are not associated with large flares, if a large flare does occur, it is inevitably associated with a CME.

Historically, flares have been defined as the localized brightenings of the chromosphere over the course of a few minutes as observed in Hα images [*Zirin*, 1988]. These Hα brightenings in the chromosphere are known as flare ribbons (see Figure 1c), and they typically occur in pairs, although more complex formations are not uncommon. More recently, the term "flares" has been used to describe the rapid onset of X-ray and UV emissions in the corona. The softer X-ray and UV emissions appear in the form of loops (see Figure 1d) with temperatures ranging from 10^5 to 3 $\times$ 10^7 K and with the UV loops nested below the X-ray ones. Cool Hα loops, corresponding to a temperature of 10^4 K, appear underneath the UV loops, and it is generally accepted that they are formed from the hot loops by a thermal condensation process [*Parker*, 1953; *Cox*, 1972]. The outermost edge of the hot X-ray loops maps to the outer edge of the ribbons [*Schmieder et al.*, 1996], while the innermost edge of the cool Hα loops maps to the inner edge of the ribbons [*Rust and Bar*, 1973]. During the course of the flare the separation between the ribbons increases, and both hot and cool loops appear to grow larger with time.

Figure 2 shows the temporal behavior at various wavelengths for a very large flare which occurred on August 28, 1966. This event had intense Hα, X-ray, and radio emissions, and it produced a high-speed shock wave which manifested itself in the chromosphere as a "Morton wave." The Morton wave is thought to be the chromospheric footprint of a fast mode MHD shock in the corona, and it is caused by a slight disturbance of the chromosphere at the location where the fast mode wave intersects the solar surface [*Dodson and Hedeman*, 1968; *Zirin and Lackner*, 1969; *Uchida*, 1970, 1974].

The Hα emission in Figure 2a comes from the two chromospheric ribbons whose appearance is the classical signature of flare onset. The Hα emission becomes quite intense within 5 min after onset but takes a long time to decay. Even after 6 hours, it still exceeds the preflare emission by almost a factor of 2. During the rapid rise phase of the Hα emission the flare ribbons move apart at a rate of more than 100 km s^{-1}, but as soon as the peak is reached, they quickly slow to a speed of the order of 4 km s^{-1}. An event of this type, lasting for many hours, is known as a "Long Duration Event" or LDE, for short. To the extent that it can be determined with imperfect observations, LDEs are always associated with a CME.

The soft X rays, which are thermal in origin, are produced by the hot > 10^7 K flare loops whose footpoints map to the Hα ribbons. Both the Hα ribbons and the soft X-ray loops persist for many hours, sometimes as long as 2 days after a really large event [*Švestka*, 1976]. Hard X rays (> 20 keV) appear only during the impulsive phase when the Hα and the soft X-ray emissions are rapidly increasing in intensity. The hard X rays are

Paper number 2000JA000005.
0148-0227/00/2000JA000005$09.00

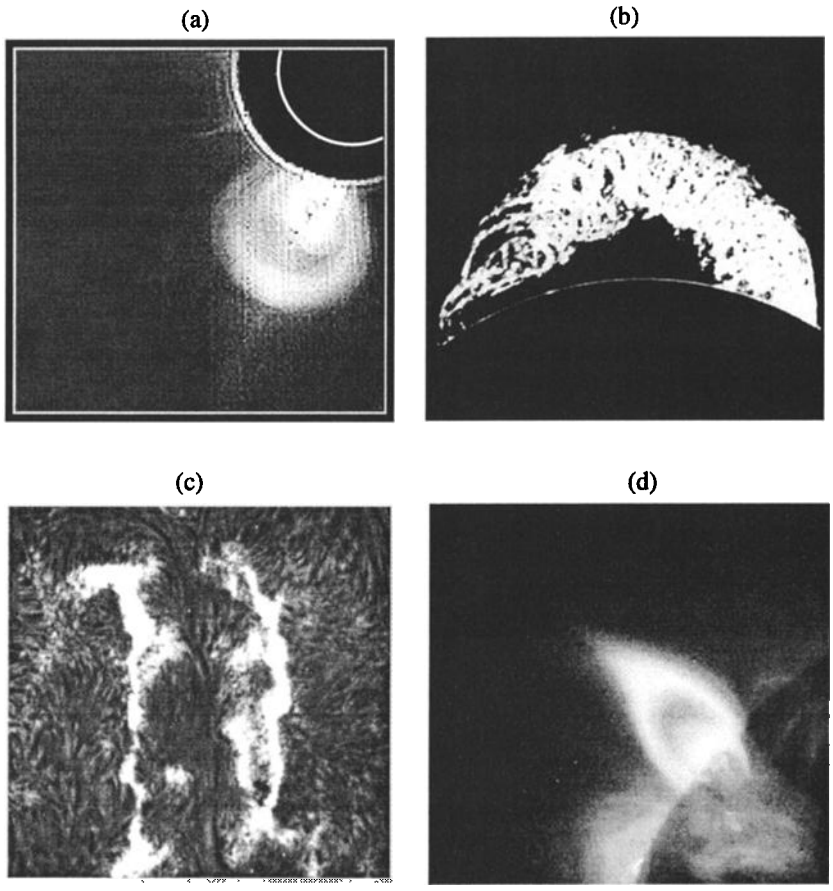

Figure 1. Solar eruptive phenomena: (a) white light coronagraph image of a coronal mass ejection (CME) containing an erupted prominence. The white circular line in the upper right-hand corner indicates the location of the Sun's surface behind the occulting disk of the instrument (August 18, 1980, SMM archive, High-Altitude Observatory). (b) Hα image of the large prominence eruption, known as "granddaddy" (June 4, 1946, High-Altitude Observatory). (c) Hα ribbons produced by a flare associated with a CME (July 29, 1973, Big Bear Solar Observatory). (d) Cusp-shaped X-ray loop system, as seen on the limb of the Sun after an eruptive event (March, 8 1999, Yohkoh archive, Institute of Space and Astronautical Science). Such posteruption loop systems are common to the three phenomena of CMEs, erupting prominences, and large flares.

generally thought to be produced by nonthermal electrons, and they are accompanied by radio emissions which support this interpretation [*Švestka and Simon*, 1969]. During the impulsive phase, γ rays and neutrons also appear, which indicates the presence of high-energy protons with energies in excess of 100 MeV.

More than half of all CMEs are associated with the eruption of prominences. Large quiescent prominences which exist outside of active regions can be quite spectacular when they erupt, as shown in Figure 1b, and they nearly always create a CME. However, the much smaller prominences that exist within active regions can also erupt, usually in association with flares, but it is not known how well they correlate with CMEs. In many cases these small prominences are difficult to identify, and their fate is often difficult to determine.

As observations have improved, it has become increasingly clear that erupting prominences outside active regions have many features typical of large flares. Like large flares, erupting prominences produce loops and ribbons which move apart in time, but unlike large flares, the ribbons are usually too faint to be seen in Hα. However, the ribbons can often be seen in the He 10830 Å line, which is a more sensitive indicator of chromospheric excitation [*Harvey and Recely*, 1984]. The eruption of a large quiescent prominence does not usually produce significant hard X-ray or γ-ray emissions, probably because it occurs in a region where the field is relatively weak (< 10 G).

High-resolution images obtained by the soft X-ray telescope on Yohkoh in 1992 have made it clear that all CMEs and prominence eruptions create faint X-ray loops which are sometimes referred to as "giant arches" [e.g., *Švestka et al.*, 1997]. These giant arches are the CME counterparts of the flare loops occurring in two-ribbon flares, but they often exhibit a pattern of motion different from that of the flare loops. Instead of continually slowing with time, the arches move upward at a rate which remains nearly constant or which may even increase with time [*Švestka*, 1996]. However, this difference can be explained by the variation of the coronal Alfvén speed with height [*Lin and Forbes*, 2000].

The interrelationship between the various features which one can associate with CMEs is shown in Figure 3. It should be kept in mind that these features are not necessarily present in all CMEs. Not all CMEs contain a prominence, nor do all CMEs have detectable chromospheric ribbons and shock waves.

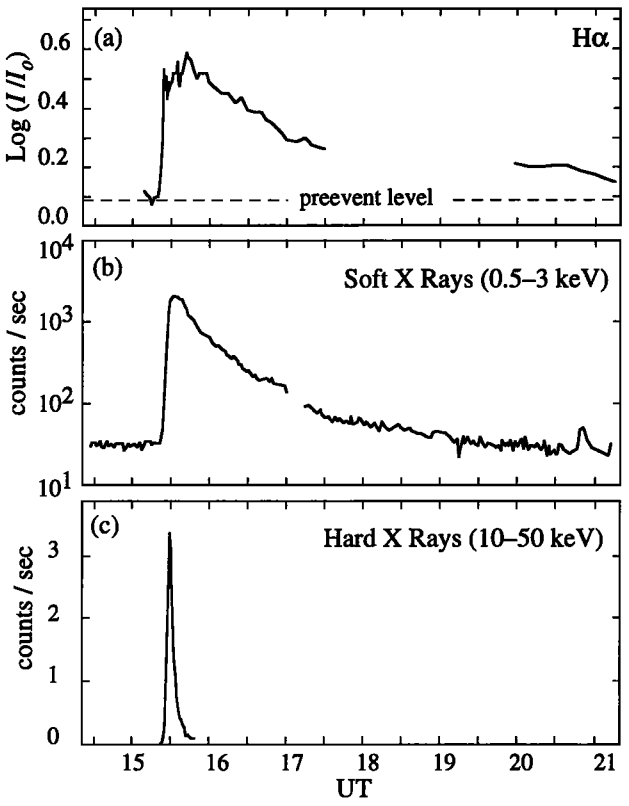

Figure 2. Time evolution of the radiation produced by a flare on August 28, 1966, which was associated with both a two-ribbon flare and a prominence eruption: (a) Hα ribbon intensity [*Dodson and Hedeman*, 1968], (b) thermal, soft X-ray emission [*Zirin and Lackner*, 1969], and (c) nonthermal, hard X-ray emission [*Arnoldy et al.*, 1968].

2. Energetics

When CMEs were first clearly identified by Skylab in 1973, many researchers assumed that they were caused by the outward expansion of hot plasma produced by a large flare. We now know that this is not the case, for several reasons. First, less than 20% of all CMEs are associated with large flares [*Gosling*, 1993]. Second, CMEs that are associated with flares often appear to start before the onset of the flare [*Wagner et al.*, 1981; *Simnett and Harrison*, 1985]. Finally, the thermal pressure produced by a flare is too small to blow open the strong magnetic field of the corona.

At the present time, the most generally accepted explanation for the cause of CMEs is that they are produced by a loss of stability or equilibrium of the coronal magnetic field [cf. *Low*, 1996]. The continual emergence of new flux from the convection zone and the shuffling of the footpoints of closed coronal field lines cause stresses to build up in the coronal field. Eventually, these stresses exceed a threshold beyond which a stable equilibrium cannot be maintained, and the field erupts. The eruption releases the magnetic energy stored in the fields associated with coronal currents, so models based on this mechanism can be thought of as "storage models."

However, from time to time, various researchers have considered the possibility that the energy source which drives CMEs and flares lies within or below the photosphere. *Sen and White* [1972], *Heyvaerts* [1974], *Hénoux* [1986], and *Kan et al.* [1983] have proposed electric dynamo models based on the fact that the photosphere is weakly ionized, having less than 10^{-4} charged carriers per neutral particle, compared to the fully ionized corona. These models invoke the same process that occurs in laboratory MHD generators when a weakly ionized plasma flows across a stationary magnetic field. However, *Melrose and McClymont* [1987] have shown that the concept of a photospheric dynamo of this type is grossly inconsistent with the observed properties of the photosphere and the way it is coupled to the regions above and below it.

A related flux injection model has been proposed by *Chen* [1989] which impulsively injects magnetic flux and power from the convection zone into the corona at CME onset. This model requires a rapid increase in the magnetic energy of the corona during the eruption, rather than a decrease as in the storage models, and it does not address the reason why the convection zone should suddenly inject flux into the corona. An analysis by *McClymont and Fisher* [1989] finds that the flux injection model requires large-scale horizontal motions that are not consistent with those that are observed. Although the photosphere is only weakly ionized, it is still an excellent conductor, and field lines there are frozen to the plasma. Thus any sudden injection of flux from the convection zone to the corona must necessarily move the photospheric plasma.

Models based on the storage of magnetic energy prior to CME onset also transfer energy from the convective zone to the corona, but this process occurs over a long time period of the order of hours to days prior to the CME. The photospheric motions are directly observed, while the buildup of current which results from them can be inferred from vector magnetograms and changes in field-aligned plasma structures (e.g., filaments and fibrils).

How much energy is required to drive a CME can be discerned from Table 1, which shows the estimated energy output of a very fast CME of moderately large size (values are from *Canfield et*

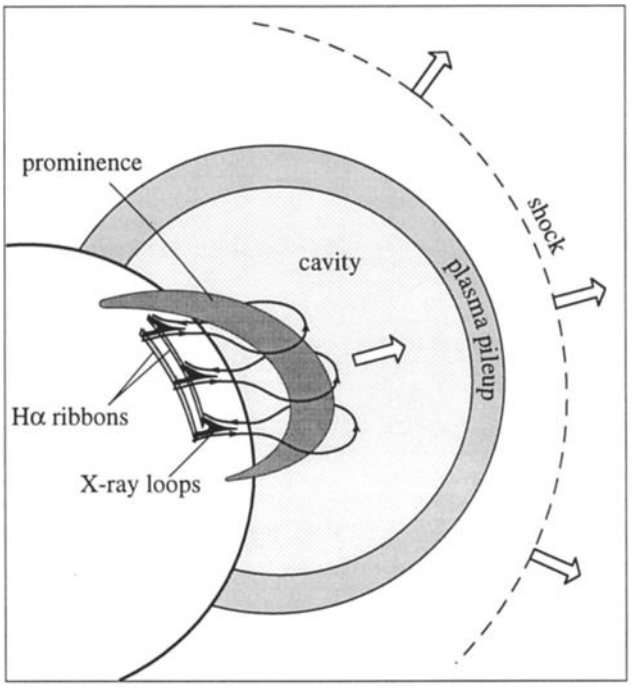

Figure 3. Schematic diagram showing the relationship between various features associated with a CME. The shaded region labeled "plasma pileup" refers to the outer circular arc seen in coronagraphs.

Table 1. Energy Requirements for a Moderately Large CME

Parameter	Value
Kinetic energy (CME, prominence, and shock)	10^{32} ergs
Heating and radiation	10^{32} ergs
Work done against gravity	10^{31} ergs
Volume involved	10^{30} cm^3
Energy density	100 ergs cm^{-3}

Table 2. Estimates of Coronal Energy Sources

Form of Energy	Observed Average Values	Energy Density ergs cm^{-3}
Kinetic ($(m_p n V^2)/2$)	$n = 10^9$ cm^{-3}, $V = 1$ km s^{-1}	10^{-5}
Thermal (nkT)	$T = 10^6$ K	0.1
Gravitational ($m_p ngh$)	$h = 10^5$ km	0.5
Magnetic ($B^2/8\pi$)	$B = 100$ G	400

al. [1980] and *Webb et al.* [1980]). By dividing the total energy requirement by the volume of the corona which erupts, we can deduce that the source must have an energy density of the order of 100 ergs cm^{-3}. Now let us compare this value with the kinetic, thermal, gravitational, and magnetic energy densities in the corona as shown in Table 2. The kinetic energy density ($m_p n V^2/2$, where m_p is the proton rest mass) is ~10^{-5} ergs cm^{-3} assuming that the coronal density n is ~10^9 cm^{-3} and that the velocity V is of the order of 1 km s^{-1} (the convective velocity of structures in the photosphere). The thermal energy density (nkT, where k is Boltzmann's constant) is ~0.1 ergs cm^{-3} since the temperature T is ~10^6 K, and the gravitational energy density ($m_p ngh$, where g is the solar surface gravity of 2.47×10^4 cm s^{-2}) is of the order of 0.5 ergs cm^{-3}, assuming that the average mass height h is ~10^{10} cm. Finally, the magnetic energy density ($B^2/8\pi$) is ~400 ergs cm^{-3} for an average field strength of 100 G, as would be appropriate for an eruption involving an active region. Thus only the magnetic energy density exceeds the required energy density of 100 ergs cm^{-3}. For reasons we will discuss shortly not all of the magnetic energy density is available to drive an eruption, but the extraction of only a quarter of it is still ample enough to account for even the most energetic of CMEs.

Because the magnetic energy density greatly exceeds the thermal and gravitational energy density in the corona, the currents associated with the magnetic energy stored there must either be force-free, as illustrated in Figure 4a, or confined to current sheets, as illustrated in Figure 4b. In other words, the energy cannot be stored as a distributed, non-force-free current in the absence of any significant gas pressure or gravitational force which could counterbalance a magnetic $\mathbf{j} \times \mathbf{B}$ force. Thus storage models for flares and CMEs are generally divided into those based on force-free currents and those based on current sheets, although as we will discuss in section 4.4, it is possible that small deviations from a perfectly force-free state might play a role in triggering some eruptions. A well-known example of a storage model utilizing a current sheet is the emerging flux model for flares shown in Figure 4b. As new flux emerges from the photosphere, it forms a current sheet as it presses against field structures that are already present. As the current in the sheet grows, it may then reach a critical threshold for the onset of a micro-instability. Although this model releases magnetic energy, it does not eject any mass or magnetic flux, so it cannot explain CMEs or prominence eruptions, but it may be applicable to small compact flares not associated with CMEs. Most CME models assume that the initial configuration is a force-free field such as the sheared arcade shown in Figure 4a. Various proposals for how such a field might erupt will be discussed in section 4.

An important constraint for CME models is the observation that the normal component of the photospheric magnetic field remains virtually unchanged during the course of the event. The slow movements of sunspots and other magnetic features in the photosphere are unaffected by the occurrence of the CME because the plasma in the photosphere is almost 10^9 times denser than the plasma in the corona where flares originate. This enormous difference in density means that it is very difficult for disturbances in the tenuous corona to have much effect on the extremely massive plasma of the photospheric layer. Field lines mapping from the corona to the photosphere are said to be "inertially line-tied," which means that the footpoints of coronal field lines are essentially stationary over the timescale of the eruption. Therefore the component of the coronal field due to photospheric field sources remains invariant during an eruption and does not contribute to the energy release.

Although the coronal magnetic field cannot be directly observed in the corona, it is possible to estimate its strength and form by taking advantage of the fact that plasma structures in the corona and chromosphere are strongly influenced by the magnetic field. By using a magnetogram of the surface field at the photosphere and assuming that contours of constant density and temperature lie along coronal field lines, it is possible to con-

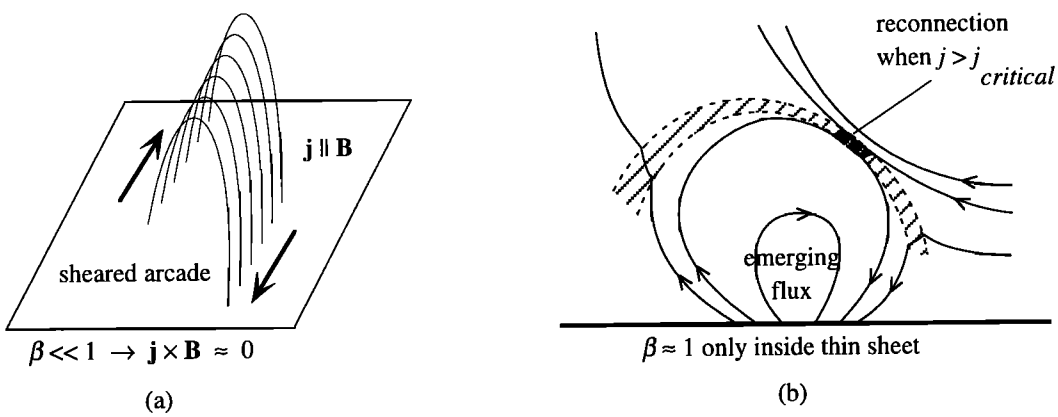

Figure 4. Examples of the two types of coronal configurations which are possible in the low-pressure environment of the corona: (a) a force-free field with a parallel current and (b) a field containing a thin current sheet.

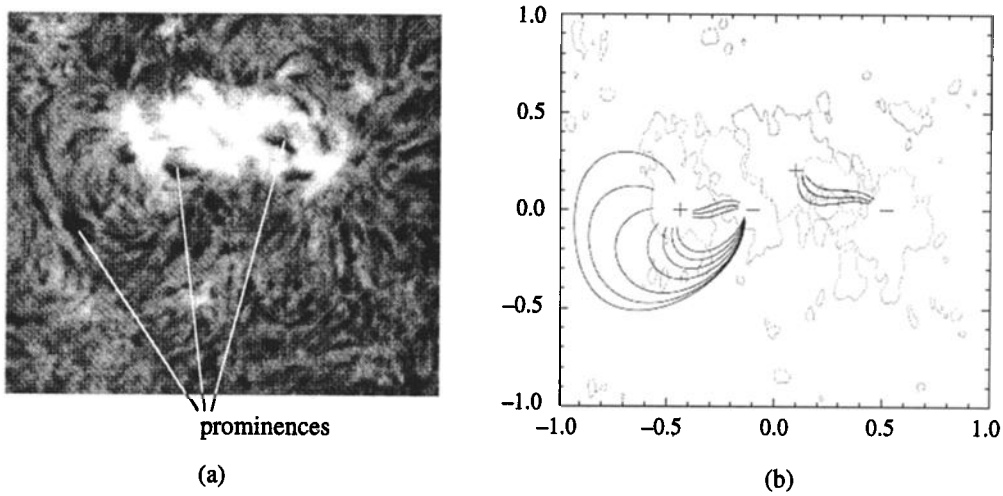

Figure 5. (a) Hα image of prominences observed by the Ottawa River Solar Observatory on July 22, 1979, and (b) a linear force-free model of the field obtained by extrapolating the normal component of the photospheric magnetic field [from *Mackay et al.*, 1997].

struct force-free models of the field as shown in Figure 5. Using this method, *Mackay et al.* [1997] have found that the ratio of the total magnetic energy (including both coronal and photospheric sources) to the potential magnetic energy (the photospheric sources alone) is ~1.3 [Mackay and Longbottom, private communication].

During a CME, magnetic field lines mapping from the ejected plasma to the photosphere are stretched outward to form an extended, open-field structure. This opening of the field creates an apparent paradox, since the stretching of the field lines implies that the magnetic energy of the system is increasing, whereas storage models require it to decrease [*Sturrock et al.*, 1984]. *Aly* [1991] and *Sturrock* [1991] have established that for a simply connected field, the fully opened field configuration always has a higher magnetic energy than the corresponding force-free field. Aly has also shown that for a simply connected magnetic field the ratio of the total magnetic energy to the potential magnetic energy is necessarily less than 2. For example, the maximum ratio for a Sun-centered dipole is 1.66 [*Low and Smith*, 1993]. The Aly-Sturrock constraint has worried many proponents of storage models because it seems to imply that such models are energetically impossible. However, there are several possible ways around the constraint. First, the magnetic field may not be simply connected and may contain knotted field lines. Second, it may contain field lines that are completely disconnected from the surface. Third, an ideal MHD eruption can still extend field lines as long as it does not open them all the way to infinity. Fourth, an ideal MHD eruption may be possible if it only opens a portion of the closed field lines. Fifth, small deviations from a perfectly force-free initial state might make a difference. Finally, a non-ideal process, specifically magnetic reconnection, might be important.

3. Origin of the Fields and Currents

The magnetic fields observed at the photosphere are quite complex, and the areas that eventually generate CMEs do not necessarily include active regions containing sunspots and strong magnetic fields. The coronal field that erupts outward during a CME has its origin in the Sun's magnetic dynamo region, which is thought to be located at the base of the convection zone (see *Glatzmaier* [1985] for references). Although many aspects of the dynamo region remain poorly understood, there is a consensus among researchers that it leads to the formation of large magnetic flux ropes that rise to the surface of the Sun because of magnetic buoyancy [*Browning and Priest*, 1986; *Low*, 1996]. As the flux ropes rise, they expand and are disrupted by the turbulent flow in which they are imbedded, so that much of the magnetic field which reaches the surface is contained in fine-scale structures concentrated within the boundary layers between supergranual convection cells. (The boundary layers are often referred to as the "network.") These cells have a characteristic length of 3×10^4 km, which may be due to the fact that helium becomes fully ionized at a depth below the photosphere which is equal to this length. (Similarly, it has been proposed that the ionization of hydrogen and the single ionization of helium give rise to the smaller characteristic length scales associated with the granulation and the meso-granulation, respectively [*Priest*, 1982].) It is now possible with the advent of helioseismology to detect the larger-scale structures before they reach the photosphere [*Kosovichev et al.*, 2000]. Once the interior field emerges through the surface into the corona, it is no longer buoyant, so it remains transfixed between the corona and the convection zone for a period of days to weeks before disappearing. Large-scale structures disappear by breaking up into increasingly smaller scale structures which eventually become too small to see with existing telescopes. Thus the eventual fate of the surface field remains unknown.

Exactly what the preeruptive magnetic field structures are in the corona and how they get that way is a subject of active research [e.g., *Krall et al.*, 1998; *Fan et al.*, 1999]. From plasma structures observed at various wavelengths, it appears that the field is in the form of a sheared arcade or half-emerged flux rope. The two possibilities are essentially indistinguishable unless the axis of the flux rope rises above the surface. From measurements of the magnetic field and flows in prominences, it is inferred that the amount of twist in the field is not large, so that if the structure is a flux rope, the number of turns within it is something between one and two [*Leroy et al.*, 1983; *Gaizauskas*, 1979; *Antiochos et al.*, 1994]. *Low* [1993] and *Gibson and Low* [2000] have argued persuasively that the region of strong magnetic field within the

flux rope should be identified with the dark cavity that is typically observed both before and after the onset of a CME (see Figures 1a and 3).

Perhaps the most important quantity to consider for any storage model is the coronal current density in the preeruptive configuration. The distribution of the current density determines how much energy is stored and whether or not the field is stable. Unfortunately, because the current density is the derivative of the magnetic field, it is even more difficult to measure accurately than the field itself.

As for the origin of the current density, there are essentially two possibilities: One is that it is created by the observed surface flows which stress the field. The other is that the current density is transported along with the field as it emerges from the convection zone [*Low*, 1996]. It is not always easy to distinguish between these two processes since the motion of the photospheric footpoints of the field line may be part of the emergence process. Many storage models assume that the corona is initially current-free and that the buildup of magnetic energy is entirely due to stressing of the coronal field by the observed photospheric motions. These motions are of the order of 1 km s^{-1} or less, and over a time period of a few days they are sufficient to store the 10^{32} ergs needed for a large CME. However, very large CMEs have sometimes been observed in regions where the photospheric motions are too slow and of too short a duration to store 10^{32} ergs. These events imply that the magnetic fields emerging from the convection zone may not be current free and may already be in a stressed state [*McClymont and Fisher*, 1989]. (This conclusion appears to confirm a statement that was once made to the author by H. Zirin that "big flares are born bad.")

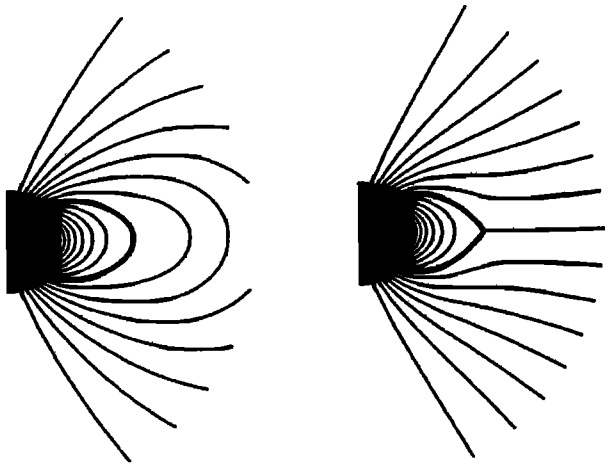

Figure 6. Two force-free magnetic configurations having the same magnetic boundary condition. (a) The field within the thick line is unsheared and potential, but the field outside it is sheared and nonpotential. (b) The field is everywhere potential except for an equatorial current sheet extending outward from the cusp. The completely closed configuration in Figure 6a has a higher magnetic energy than the partly opened configuration in Figure 6b [after *Wolfson and Low*, 1992].

4. Illustrative Models

In this section we discuss some representative models which are all based on the principle that CMEs are powered by the sudden release of magnetic energy stored in the corona. Four different classes of models can be distinguished: First is a class of force-free models which attempt to explain the eruption solely in terms of an ideal MHD process. Second is a class of models that invoke resistive MHD processes such as magnetic reconnection to trigger the eruption. Third is a class of hybrid models which initiate the eruption by a purely ideal MHD process but require the nonideal process of magnetic reconnection in order to sustain the eruption. Finally is a fourth class of models which supposes that the small deviations from a completely force-free field, caused by gravity or gas pressure, may play a significant role in the initiation of an eruption.

4.1. Ideal MHD Models

The class of ideal MHD models deals with processes that require no dissipation or diffusion of the magnetic field to operate. Although a dissipative process like reconnection may occur, it is assumed to play no role in the eruption of the field. Models of this type are severely restricted by the Aly-Sturrock constraint discussed in section 2, namely, that a completely opened magnetic field always has a higher magnetic energy than the corresponding closed state. However, one way around this constraint is to suppose that during a CME eruption only a portion of the total field is opened, while the remainder remains closed [*Wolfson*, 1993].

Wolfson and Low [1992] have shown explicitly that a partly opened state can exist which has a lower magnetic energy than an initial fully closed state with the same photospheric boundary condition. Their initial and final configurations with this property are shown in Figure 6. Unfortunately, their method of solution does not allow them to determine whether a transition from the closed state to the open state is possible in the absence of reconnection, so at the present time there is still no model which demonstrates that a partly open magnetic field can be achieved solely by a loss of ideal MHD equilibrium or stability. Perhaps further exploration of the configurations considered by Wolfson and Low could be carried out using numerical methods.

4.2. Resistive MHD Models

Another way to get around the Aly-Sturrock constraint is to appeal to a nonideal process, such as magnetic reconnection, since the constraint only applies to strictly ideal MHD. How such a process might work is shown in Figure 7, which is taken from a numerical calculation by *Mikić and Linker* [1994]. From t = 0 to 540 τ_A the arcade is sheared with the resistivity as near to zero as possible (where τ_A is the Alfvén scale time of the global structure). After 540 τ_A the shearing is stopped, and the resistivity is instantaneously increased to a value which gives an effective magnetic Reynolds number of ~10^4. This increase leads to reconnection and the formation of a flux rope which is expelled outward, away from the Sun. If the resistivity does not increase, then the configuration gradually (i.e. quasi-statically) opens up without any sudden eruption of the field.

The magnetic force which drives the flux rope outward originates from two different effects: The first is the compression of the magnetic field between the flux rope and the solar surface. This force is due to the inertial line-tying at the photosphere, and it is sometimes referred to as the diamagnetic force [*Yeh*, 1983]. The second is the curvature force caused by the pinching of poloidal field at the inner edge of the curved flux rope [*Shafranov*, 1966]. Of these two forces, the curvature force is the more important because it acts over a much longer range than the

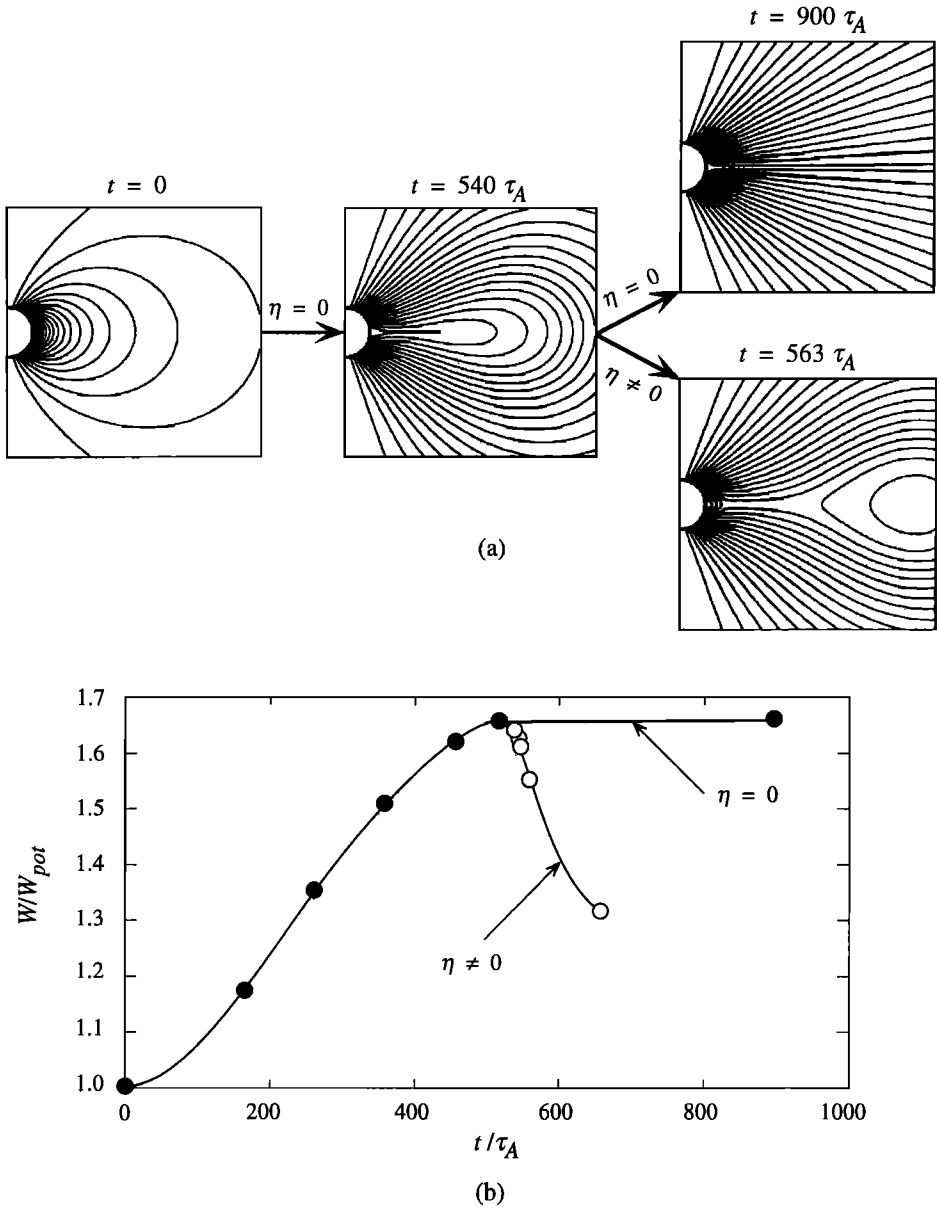

Figure 7. (a) Quasi-static evolution of an axially symmetric arcade which is sheared by rotating the Northern and Southern Hemispheres of the Sun in opposite directions. The initial field at $t = 0$ is a Sun centered dipole which evolves into the force-free field shown at $t = 540\ \tau_A$. After a rotation of 126 °, the field becomes fully opened at $t = 900\ \tau_A$, if the magnetic resistivity η remains zero. However, an eruption occurs at $t = 563\ \tau_A$ if η is suddenly increased. (b) The corresponding evolution of total energy divided by the potential energy [after *Mikić and Linker*, 1994].

diamagnetic force, which quickly dies away as the flux rope moves away from the Sun.

In order for *Mikić and Linker's* [1994] model to explain CMEs, the reconnection rate must undergo a sudden transition. Prior to the eruption it must be much slower than the timescale of the photospheric motions so that energy can be stored in the coronal currents. After the eruption it must be fast so that energy can be released rapidly. Thus a complete model of the eruption process must explain why the reconnection rate suddenly changes at the time of the eruption. There are several possible mechanisms which could do this. For example, if the current sheet is subject to the tearing mode instability, then reconnection will not occur until the length of the current sheet becomes longer than $\sim 2\pi$ times its width [*Furth et al.*, 1963]. Alternatively, as the current sheet builds up, its current density may exceed the threshold of a micro-instability, which creates an anomalous resistivity [*Galeev and Zelenyi*, 1975; *Heyvaerts and Priest*, 1976]. The anomalous resistivity subsequently triggers rapid reconnection and the ejection of a flux rope.

Another example of a model which requires a nonideal process is the model developed by *Antiochos et al.* [1999] which has the spherical quadrupolar geometry shown in Figure 8. As the central arcade straddling the equator is sheared, it pushes upward against the x line above it and creates a curved, horizontal current layer. In the absence of gas pressure or resistivity this layer is an infinitely thin sheet, and it confines the central arcade so that it

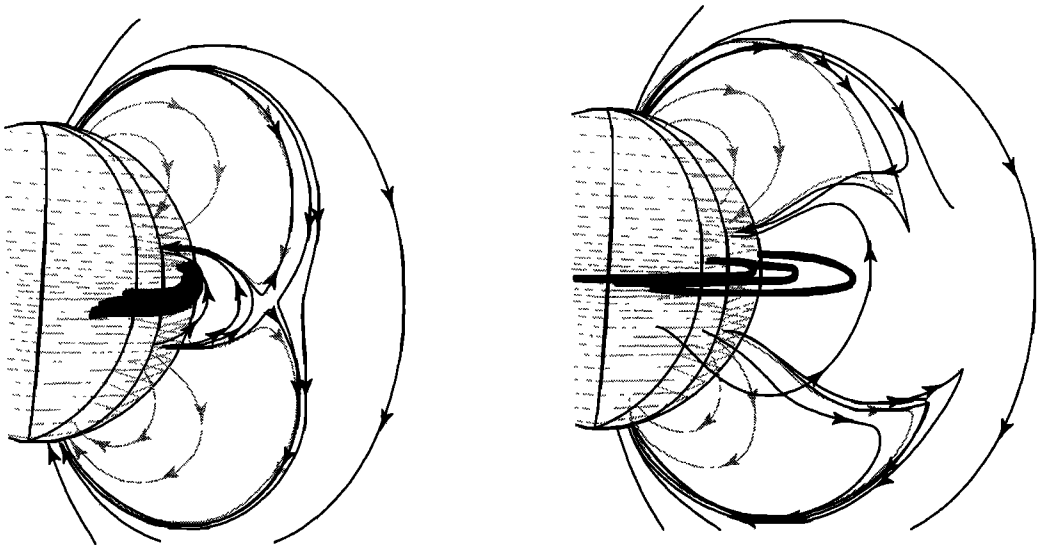

(a) (b)

Figure 8. Magnetic field configurations in the model by *Antiochos et al.* [1999] at (a) an early time and (b) a late time. Because the field is symmetric about the axis of rotation, only one side is shown. A force-free current is created by shearing the arcade field (thick lines) at the equator, but a current layer horizontal to the solar surface is also created as the sheared region bulges outward. Reconnection of the field lines in this layer allows the sheared field lines to open outward to infinity (figure templates courtesy of S. Antiochos).

cannot open. When gas pressure and reconnection are included, the current which develops at the x line is initially quite diffuse, so rapid reconnection does not occur at first. However, as the shear increases, the diffuse current evolves into a thin current sheet which eventually undergoes rapid reconnection.

Antiochos et al. [1999] have rigorously shown that the magnetic energy stored in the final, partly opened state is less than the magnetic energy stored in the preeruptive state. This result is similar to the one of *Wolfson and Low* [1992] discussed above, except that here there is a clear description of the transition from the closed state to the partly opened state. The precise nature of the transition from slow reconnection to rapid reconnection in the model still remains to be determined.

4.3. Ideal Resistive Hybrids

The resistive model of *Mikić and Linker* [1994] described in section 4.2 utilizes a sudden change in the rate of reconnection to produce a dynamic eruption. If such a change does not occur, then the system just evolves quasi-statically at the rate set by the slow evolution of the photospheric field. Although the onset of a micro-instability is one way to change the reconnection rate rapidly, another way is to have an ideal MHD process suddenly create a current sheet.

An example how this process would work is illustrated in Figures 9 and 10, which show an idealized flux rope model with the same axial symmetry as that assumed by *Mikić and Linker* [1994]. The particular model shown in Figures 9 and 10 was derived by *Lin et al.* [1998], but the basic concept was developed earlier by *Van Tend and Kuperus* [1978], *Molodenskii and Fillipov* [1987], and *van Ballegooijen and Martens* [1989], among others. Initially, the flux rope is suspended in the corona by a balance between magnetic tension, compression, and curvature forces (the latter caused by the pinching of the poloidal field at the inner edge of the flux rope). However, this balance cannot be maintained if the photospheric source of the coronal field is reduced below a critical value. When the balance is lost, the flux rope jumps to an equilibrium at a higher height as shown in Figure 10, and a relatively small fraction (< 10%) of the stored magnetic energy is released. The new equilibrium contains a vertical current sheet located below the flux rope (see. Figure 9), and unless reconnection occurs in this sheet, the flux rope cannot escape into interplanetary space. Just how fast the reconnection rate has to be in order for a smooth escape to occur has been estimated by *Lin and Forbes* [2000] for a two-dimensional configuration with translational symmetry (i.e., a Cartesian system). They show that a smooth escape is possible if the inflow Alfvén Mach number into the current sheet exceeds ~0.005. The actual value of this number inferred from the observations is ~0.025 [*Poletto and Kopp*, 1986], so a smooth escape is to be expected.

The quasi-static evolution in Figures 9 and 10 before eruption occurs is accomplished in a highly idealized manner by reducing the strength of the photospheric field (in this case a simple Sun-centered dipole). This reduction requires the footpoints of field lines in the Northern and Southern Hemispheres to migrate toward the equator and reconnect so that the work done in moving these footpoints is transferred to the coronal currents via a Poynting flux. Although colliding polarities which reconnect might conceivably be a source of some eruptions [*Zirin*, 1988], any photospheric boundary condition which changes the relative strength of the repulsive and attractive forces acting on the flux rope will suffice. For example, in the two-dimensional analysis by *Forbes and Priest* [1995] a loss of equilibrium is triggered by simply moving the photospheric sources closer to one another without reconnection or a reduction of the photospheric field.

Because of the assumed symmetry, the flux rope in Figure 9 is a torus which encircles the Sun, and thus it contains field lines

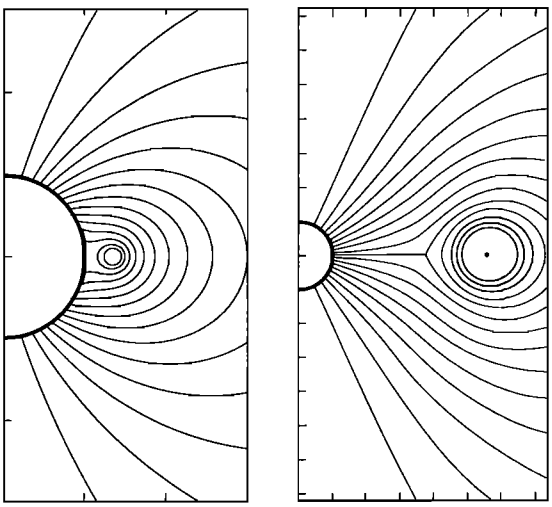

Figure 9. Axially symmetric flux rope model showing the ideal MHD transition from (a) the high-energy equilibrium state before eruption to (b) the low energy equilibrium state after eruption. The difference in scale between the figures 9a and 9b is indicated by the difference in the size of the Sun. Initially, the radius of the flux rope is assumed to be ~10^4 km. The field lines remain closed throughout, but the configuration formed afterward contains a current sheet. The flux rope can only escape in a smooth manner if the reconnection process in the sheet is fast enough [after *Lin et al.*, 1998].

which are not attached to the solar surface as shown in Figure 9. It has been argued by *Antiochos et al.* [1999] that the flux rope model will not work once its ends are anchored (i.e., line-tied) to the photosphere. However, their argument assumes that the jump in the flux rope model involves a violation of the Aly-Sturrock constraint which, as originally formulated, does not include configurations with unattached field lines. In fact, one can show rigorously that for this particular model the energy of the open state exceeds all other states [see *Lin et al.*, 1998], a result which suggests that the Aly-Sturrock limit may also apply to at least some configurations with detached field lines. The important aspect of *Lin et al.'s* [1998] model, which is not present in the models of *Mikić and Linker* [1994] or *Antiochos et al.* [1999], is that slowly changing the photospheric field can lead to the sudden formation of a current sheet. (A process often referred to as a "catastrophe" according to the usage introduced by *Thom* [1972].)

The maximum total magnetic energy which can be stored in this flux rope model before equilibrium is lost is 1.53 times the energy of the potential field, less than the limiting value of 1.66 for the fully opened field. The way the model gets around the Aly-Sturrock constraint is by invoking the nonideal process of magnetic reconnection. The only role of the ideal MHD transition is the sudden creation of a current sheet, and this process replaces the onset of a micro-instability that has been invoked in other resistive MHD models [e.g., *Mikić and Linker*, 1994].

Whether the catastrophic process which creates the current sheet will still work when the ends of the flux rope are tied to the photosphere remains an unanswered question. However, it is likely that it will for the following reason: When the ends of the flux rope are tied, an upward displacement of a middle portion of the flux rope constitutes an ideal MHD kink. Thus the relevant question to consider is whether the configuration can become kink unstable. Since the kink instability is an inherently three-dimensional process, it can be quite difficult to obtain stability criteria for it in a complex configuration involving a curved flux rope, a line-tying boundary, and a nonuniform external field. In the absence of line-tying or external fields, a straight flux rope is always unstable no matter what the current distribution is inside it [*Anzer*, 1968]. A straight, isolated flux rope of finite length can be stabilized by anchoring its ends at fixed boundaries but only if the twist is less than a critical value [*Hood and Priest*, 1981]. For a force-free flux rope with a uniform twist the critical value is 3.3 π corresponding to 1.7 turns of the flux rope between the two boundaries [*Hood and Priest*, 1979], but this number may be higher or lower depending on the distribution of current within the flux rope.

If the flux rope is twisted beyond the critical number of turns, it becomes unstable and dynamically jumps to a lower energy state [*Arber et al.*, 1999] which necessarily contains a current sheet [*Bhattacharjee and Wang*, 1991]. It seems unreasonable to suppose that curving the flux rope and adding an external background field would cause the line-tying to become so efficient that the flux rope would become unconditionally stable no matter how much it is twisted. If this were true, then gradually reducing the curvature and external field to zero would not recover the result of *Hood and Priest* [1979].

Titov and Démoulin [1999] have recently analyzed the special case of a circular flux rope which is imbedded in a line-tying surface as shown in Figure 11a. The outward curvature force acting on the rope is counterbalanced by the field from two point magnetic charges buried at a depth $z = -d$ below the surface and located at $x = \pm L$ as indicated in Figure 11. In addition to the external field generated by the point charges, there is also a contribution from an infinitely long line current which coincides with the x axis. The field produced by this line current exerts no force

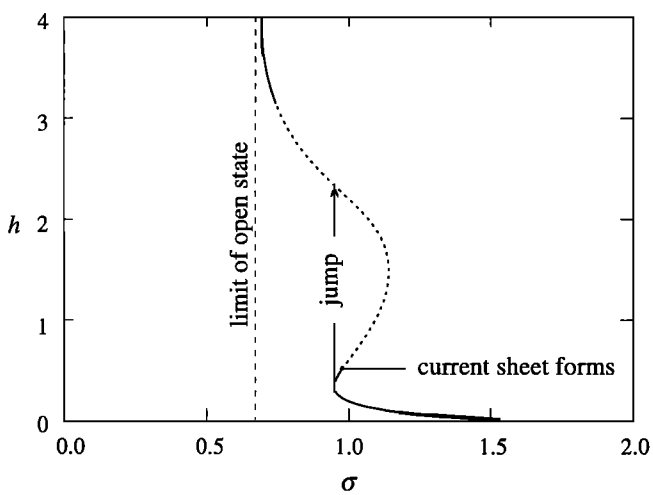

Figure 10. The equilibrium height h of the flux rope shown in Figure 9 in units of the solar radius as function of the strength, σ, of the Sun centered dipole in normalized units. The dotted portion of the curve indicates an extrapolation between the asymptotic solution (upper portion of curve) and the no-current-sheet solution (lower portion). When the field strength σ is slowly reduced to 0.95, the flux rope undergoes a dynamic jump to a new state containing a current sheet. Upon further reduction of σ to 0.74 (dashed line), the field evolves quasi-statically to the open state [after *Lin et al.*, 1998].

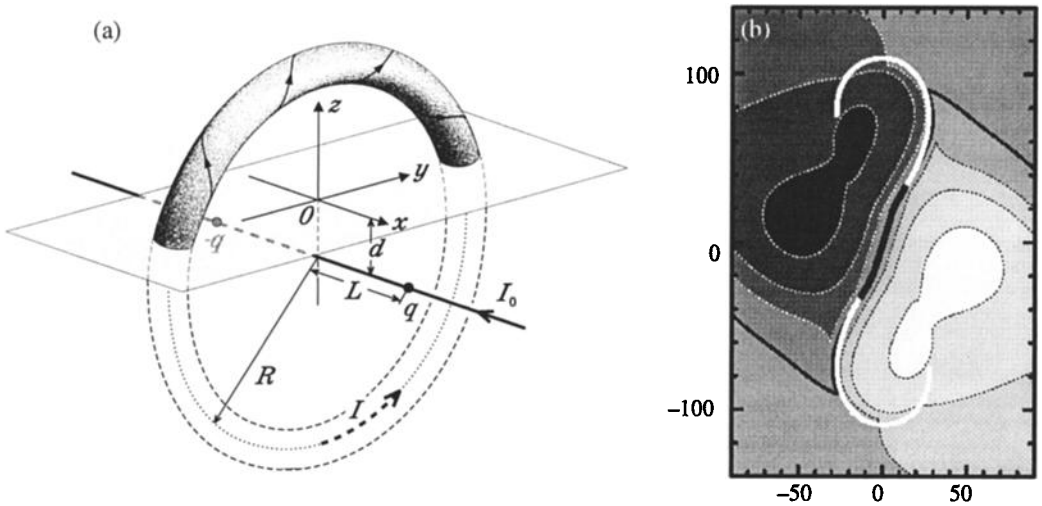

Figure 11. Line-tied flux rope model of *Titov and Démoulin* [1999]: (a) three-dimensional view showing the relation of the flux rope (shaded torus) to the background field sources at a depth d below the surface. These sources are point magnetic charges $\pm q$ located at $x = \pm L$ and a line current running along the x axis. (b) normal components of the surface magnetic field with regions of opposite polarity indicated by dark and light tones. The polarity inversion line is indicated by a thin black line, while the bald-patch region is indicated by a thick black line. The photospheric traces of the magnetic separatrices are indicated by the white lines.

on the flux rope, and its purpose is to make the overall field structure more nearly resemble that occurring in the corona. Without the field from the line current the field lines at the surface of the flux rope are purely poloidal, and they have an infinite number of turns in a finite length. This is quite unrealistic because a variety of observations indicate that the maximum number of turns on any field line is probably less than two (see section 3). Incorporating the line current field eliminates this problem by creating a strong toroidal field which ensures that no field lines are highly twisted. By adjusting the strength of the line current one can achieve a reasonable amount of twist everywhere as shown in Figure 11b.

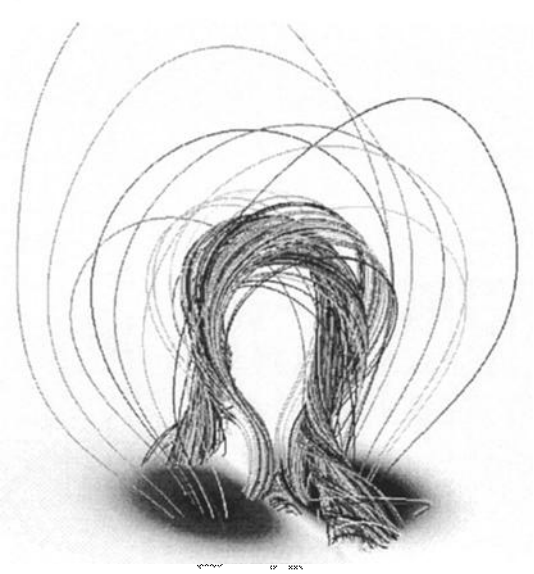

Figure 12. Magnetic field configuration formed by reconnecting the photospheric footpoints of a fully three-dimensional arcade (from the simulation by *Amari et al.* [2000]).

Titov and Démoulin [1999] have also considered the stability of their configuration and assert that it is unstable if the large radius, R, of the flux rope (Figure 11a) exceeds $\sqrt{2}\,L$ in the limit that d is small. Although they do not prove this result rigorously, they are able to establish that the configuration has equilibrium properties similar to the completely symmetric configuration shown in Figure 9.

There is also a fully three-dimensional simulation by *Amari et al.* [2000] which shows how a flux rope can be formed by reconnecting the photospheric footpoints of a sheared arcade. Such a process was suggested 10 years ago by *van Ballegooijen and Martens* [1989] and later simulated in two dimensions by *Inhester et al.* [1992]. In the simulation of Amari et al. the reconnection of the photospheric field leads to the sudden formation of a flux rope with a vertical current sheet below (see Figure 12). However, it is not at all clear if the transition to this state constitutes a true catastrophe, because the photospheric boundary condition in the simulation is changed at a rate which is too rapid to be considered quasi-static. Thus there is still no convincing demonstration at the present time that a realistic eruption can be modeled using a line-tied flux rope configuration like that shown in Figure 11.

Even if it should turn out that a simple curved flux rope cannot produce a realistic eruption, there are other closely related configurations that may be able to do so. *Gibson and Low* [1998, 2000] have shown that the overall appearance of CMEs both before and after eruption can be modeled quite well using the same type of force-free fields as occurs in spheromaks, but the equilibrium and stability properties of these fields in the presence of a line-tying surface remain to be determined.

4.4. Non-Force-Free Models

The restriction imposed by the Aly-Sturrock constraint can be sidestepped if the initial configuration is not force-free. It is generally supposed that the coronal magnetic field is nearly force-free because of the dominance of the magnetic energy over all

other forms (see Table 2), but it is possible that small deviations from a purely force-free field might play a role in triggering an eruption.

Low [1999] has pointed out that total magnetic energy in the corona can be expressed as

$$\int_{r>R_o} \frac{B^2}{8\pi} dV = \int_{r=R_o} \frac{R_o}{8\pi}\left(B_r^2 - B_\theta^2 - B_\phi^2\right) - p\, dS$$

$$+ \int_{r>R_o} \frac{\rho G M_o}{r} - 3p\, dV,$$

where **B** is the total coronal magnetic field with spherical components B_r, B_θ, and B_ϕ, p is the coronal gas pressure, ρ is the coronal density, G is the universal constant of gravitation, M_o is the solar mass, dV is the differential volume element, R_o is the solar radius, and dS is the differential surface element. The above expression is obtained from the MHD virial theorem (see *Chandrasekhar* [1961] or *Priest* [1982]), and it expresses the coronal magnetic energy in terms of the surface magnetic field and gas pressure and the volumetric gravitational and thermal energy in the corona.

If the gravitational and thermal energy are ignored, the field is force-free, and the magnetic energy is given entirely in terms of an integral over the components of the surface field. From the form of the integrand one sees that the value of this integral has an upper bound given by integrating over the radial component B_r. Since the line-tying of the field at the surface makes B_r invariant there, the amount of total magnetic energy must be less than that obtained by integrating the radial component of the potential field over all space. In other words, the maximum total magnetic energy of a force-free field in the corona cannot be more than about double that of the potential field, one of Aly's results (see section 2).

If gravity is important but pressure is not, then the magnetic field is no longer force-free, and it is possible to increase the magnetic energy stored in the corona above its force-free limit by an amount equal to the gravitational potential energy:

$$\int_{R_o}^{\infty} \frac{\rho G M_o}{r} dV \approx \frac{G M_c M_o}{R_o},$$

where M_c is the coronal mass supported by the field. This gravitational energy is essentially the same as that listed in Table 1, but it is a factor of R_o/h (~7) greater than that considered in Table 2, which is the energy gained if an object falls to the surface from a coronal scale height h rather than infinity. Thus the gravitational energy could allow the stored magnetic energy to exceed its maximum force-free value by as much as 10%.

Some of the cool plasma in an erupting prominence is often seen to fall back to the surface, which suggests that a CME might be triggered if the magnetic field slowly evolves to a critical point where it can no longer support the prominence [*Low*, 1999]. In other words, the weight of the prominence acts as a lid which allows the magnetic energy to increase above the open limit, and when the lid is suddenly removed, the field springs outward. Even if the draining of the material is not sufficient to open the field, it could, nevertheless, lead to the formation of a current sheet. However, many CMEs do not appear to contain any prominence material, so it seems unlikely that such a mechanism could account for all CMEs.

The effects of both pressure and gravity have been considered by *Low and Smith* [1993], *Wolfson and Dlamini* [1997], and *Wolfson and Saran* [1998]. As can be seen from the virial theorem, pressure reduces the magnetic energy that can be stored in the corona, but unlike gravity, pressure can itself propel material outward given the appropriate gradient. However, the problem still remains that the thermal energy density associated with pressure in the lower corona is so small that it is difficult for it to have a significant effect.

5. Summary

Many models have been developed to explain the appearance or propagation of CMEs, but very few have been developed which really explain the exact nature of the mechanism (or mechanisms) which triggers them. For example, several of the models we have discussed here propose that CMEs are triggered by the onset of a micro-instability which leads to a sudden enhancement of the resistivity in a current sheet, but they do not actually prescribe the process which produces the micro-instability. What is required is a mechanism that will cause a sudden transition from the preonset quasi steady state to the postonset dynamic state. The mechanism which triggers the eruption need not involve a micro-instability. There are models, such as the flux rope model discussed in section 4.3, which use an ideal MHD catastrophe to form a current sheet on a timescale of the same order as the Alfvén timescale of the system (typically 10–100 s in the corona).

At the present time, there is a general (but not universal) consensus that the onset mechanism involves the release of the free magnetic energy associated with currents flowing in the corona. However, there is no consensus about the mechanism which releases this energy. Nevertheless, as observations and general interest in CMEs increase, there is every reason to hope that the issue may be resolved within a few years.

Acknowledgments. The author thanks Boon-Chye Low and Spiro Antiochos for their helpful comments on the original manuscript and also Nancy Crooker and Janet Luhmann for their invitation to present this work at the Solar and Heliospheric INterplanetary Environment (SHINE) meeting held June 14-17, 1999, in Boulder, Colorado. This work was supported by NASA grants NAG5-4856 and NAG5-1479 to the University of New Hampshire and NAS 8-37334 to the Lockheed-Martin Corporation.

Janet G. Luhmann thanks Richard Wolfson and Spiro K. Antiochos for their assistance in evaluating this paper.

References

Aly, J. J., How much energy can be stored in a three-dimensional force-free field?, *Astrophys. J., 375*, L61-L64, 1991.

Amari, T., J. F. Luciani, Z. Mikic, and J. Linker, A twisted flux rope model for coronal mass ejections and two-ribbon flares, *Astrophys. J., 529*, L49-L52, 2000.

Antiochos, S. K., R. B. Dahlburg, and J. A. Klimchuk, The magnetic field of solar prominences, *Astrophys. J., 420*, L41-L44, 1994.

Antiochos, S. K., C. R. DeVore, and J. A. Klimchuk, A model for solar coronal mass ejections, *Astrophys. J., 510*, 485-493, 1999.

Anzer, U., The stability of force-free magnetic fields with cylindrical symmetry in the context of solar flares, *Sol. Phys., 3*, 298-315, 1968.

Arber, T. D., A. W. Longbottom, and R. A. M. van der Linden, Unstable coronal loops: Numerical simulations with predicted observational signatures, *Astrophys. J., 517*, 990-1001, 1999.

Arnoldy, R. L., S. R. Kane, and J. R. Winkler, The observation of 10-50 kev solar flare particles, in *Structure and Development of Solar Active Regions: IAU Symposium 35*, edited by K. O. Kiepenheuer, pp. 490-509, D. Reidel, Norwell, Mass., 1968.

Bhattacharjee, A., and X. Wang, Current sheet formation and rapid reconnection in the solar corona, *Astrophys. J.*, *372*, 321-328, 1991.

Browning, P. K., and E. R. Priest, The shape of buoyant coronal loops in a magnetic field and the eruption of coronal transients and prominences, *Sol. Phys.*, *106*, 335-351, 1986.

Canfield, R. C., C.-C. Cheng, K. P. Dere, G. A. Dulk, D. J. McLean, R.D. Robinson Jr., E. J. Schmahl, and S. A. Schoolman, Radiative energy output of the 5 September 1973 flare, in *Solar Flares: A Monogram From the Skylab Solar Workshop*, edited by P. A. Sturrock, pp. 451-469, Colo. Assoc. Univ. Press, Boulder, Colo., 1980.

Chandrasekhar, S., *Hydrodynamic and Hydromagnetic Stability*, Dover, Mineola, N. Y., 1961.

Chen, J., Effects of toroidal forces in current loops embedded in a background plasma, *Astrophys. J.*, *338*, 453-470, 1989.

Cox, D. P., Theoretical structure and spectrum of a shock wave in the interstellar medium: The Cygnus Loop, *Astrophys. J.*, *178*, 143-157, 1972.

Dodson, H. W., and E. R. Hedeman, The proton flare of August 28, 1966, *Sol. Phys.*, *4*, 229-239, 1968.

Fan, Y., E. G. Zweibel, M. G. Linton, and G. H. Fisher, The rise of kink-unstable magnetic flux tubes and the origin of δ-configuration sunspots, *Astrophys. J.*, *521*, 460-477, 1999.

Forbes, T. G., and E. R. Priest, Photospheric magnetic field evolution and eruptive flares, *Astrophys. J.*, *446*, 377-389, 1995.

Furth, H. P., J. Killeen, and M. N. Rosenbluth, Finite-resistivity instabilities of a sheet pinch, *Phys. Fluids*, *6*, 459-484, 1963.

Gaizauskas, V., Braided structures observed in flare-associated H alpha filaments, in *Physics of Solar Prominences: IAU Colloquium 44*, edited by E. Jensen, P. Maltby, and F. Q. Orrall, pp. 272-275, Oslo Univ. Press, Oslo, 1979.

Galeev, A. A., and L. M. Zelenyi, Metastable states of diffuse neutral sheet and the substorm explosive phase, *JETP Letts.*, *22*, 170-172, 1975.

Gibson, S. E., and B. C. Low, A time-dependent three-dimensional magnetohydrodynamic model of the coronal mass ejection, *Astrophys. J.*, *493*, 460-473, 1998.

Gibson, S. E., and B. C. Low, Three-dimensional and twisted: An MHD interpretation of on-disk observational characteristics of coronal mass ejections, *J. Geophys. Res.*, in press, 2000.

Glatzmaier, G. A., Numerical simulations of stellar convective dynamos, 3, At the base of the convection zone, *Geophys. Astrophys. Fluid Dyn.*, *31*, 137-150, 1985.

Gosling, J. T., Coronal mass ejections and magnetic flux ropes in interplanetary space, in *Physics of Magnetic Flux Ropes, Geophys. Monogr. Ser.*, vol. 58, edited by C. T. Russell, E. R. Priest, and L. C. Lee, pp. 343-364, AGU, Washington, D.C., 1990.

Gosling, J. T., The solar flare myth, *J. Geophys. Res.*, *98*, 18,937-18,949, 1993.

Harvey, K. L., and F. Recely, He I 10830 observations of the 3N/M4.0 flare of 4 September, 1982, *Sol. Phys.*, *91*, 127-139, 1984

Hénoux, J.-C., Dynamo theories of solar flares, in *Solar Maximum Analysis*, edited by V. E. Stepanov and V. N. Obridko, pp 109-122, VNU Sci. Press, Utrecht, 1986.

Heyvaerts, J., Coronal electric currents produced by photospheric motions, *Sol. Phys.*, *38*, 419-437, 1974.

Heyvaerts, J., and E. R. Priest, Thermal evolution of current sheets and the flash phase of solar flares, *Sol. Phys.*, *47*, 223-231, 1976

Hood, A. W., and E. R. Priest, Kink instability of solar coronal loops as the cause of solar flares, *Sol. Phys.*, *64*, 303-321, 1979.

Hood, A. W., and E R. Priest, Critical conditions for magnetic instabilities in force-free coronal loops, *Geophys. Astrophys. Fluid Dyn.*, *17*, 297-318, 1981.

Hundhausen, A J., The origin and propagation of coronal mass ejections, in *Proceedings of the Sixth International Solar Wind Conference*, vol. 1, edited by V.J. Pizzo, T. Holzer, and D G. Sime, National Center for Atmospheric Research Technical Note, NCAR TN-306+Proc., pp. 181-241, Boulder, Colo., 1988.

Inhester, B., J. Birn, and M. Hesse, The evolution of line-tied coronal arcades including a convergent footpoint motion, *Sol. Phys*, *138*, 257-281, 1992.

Kan, J. R., S.-I. Akasofu, and L. C. Lee, A dynamo theory of solar flares, *Sol. Phys.*, *84*, 153-167, 1983.

Kosovichev, A. G., T. L. Duvall, and P. H. Scherrer, Time-distance inversion methods and results - (invited review), *Sol. Phys.*, *192*, 159-176, 2000.

Krall, J., J. Chen, R. Santoro, D. S. Spicer, S. T. Zalesak, and P. J. Cargill, Simulation of buoyant flux ropes in a magnetized solar atmosphere, *Astrophys. J.*, *500*, 992-1002, 1998.

Leroy, J. L., V. Bommier, and S. Sahal-Brechot, The magnetic field in the prominences of the polar crown, *Sol. Phys.*, *83*, 135-142, 1983.

Lin, J., and T. G. Forbes, Effects of reconnection on the coronal mass ejection process, *J. Geophys. Res.*, *105*, 2375-2392, 2000.

Lin, J., T. G. Forbes, P. A. Isenberg, and P. Démoulin, The effect of curvature on flux-rope models of coronal mass ejections, *Astrophys. J.*, *504*, 1006-1019, 1998.

Low, B. C., Magnetohydrodynamic processes in the solar corona: Flares, coronal mass ejections, and magnetic helicity, *Phys. Plasmas*, *1*, 1684-1690, 1993.

Low, B. C., Solar activity and the corona, *Sol. Phys*, *167*, 217-265, 1996.

Low, B. C., Coronal mass ejections, flares and prominences, in *Solar Wind Nine*, edited by S. R. Habbal et al., pp. 109-114, AIP, Woodbury, N. Y., 1999.

Low, B. C., and D. F. Smith, The free energies of partially open coronal magnetic fields, *Astrophys. J.*, *410*, 412-425, 1993.

Mackay, D. H., V. Gaizauskas, G. J. Rickard, and E. R. Priest, Force-free and potential models of a filament channel in which a filament forms, *Astrophys. J.*, *486*, 534-549, 1997.

McClymont, A. N., and G. H. Fisher, On the mechanical energy available to drive solar flares, in *Solar System Plasma Physics, Geophys. Monogr. Ser*, vol. 54, edited by J. H. Waite Jr., J. L. Burch, and R. L. Moore, pp. 219-225, AGU, Washington, D.C., 1989.

Melrose, D. B., and A. N. McClymont, The resistances of the photosphere and of a flaring coronal loop, *Sol. Phys.*, *113*, 241-246, 1987.

Mikić, Z., and J. A. Linker, Disruption of coronal magnetic field arcades, *Astrophys. J.*, *430*, 898-912, 1994.

Molodenskii, M. M., and B. P. Filippov, Rapid motion of filaments in solar active regions, II, *Sov. Astron. (Engl.. Transl.)*, *31*, 564-568, 1987.

Parker, E. N., Instability of thermal fields, *Astrophys. J.*, *117*, 431-436, 1953.

Poletto, G., and R. A. Kopp, Macroscopic electric fields during two-ribbon flares, in *The Lower Atmosphere of Solar Flares*, edited by D. F. Neidig, pp. 453-465, NSO, Sunspot, N. M., 1986

Priest, E. R , *Solar Magnetohydrodynamics*, D. Reidel, Norwell, Mass., 1982.

Rust, D. M., and V. Bar, Magnetic fields, loop prominences and the great flares of August, 1972, *Sol. Phys.*, *33*, 445-459, 1973.

Schmieder, B., P. Heinzel, L. van Driel-Gesztelyi, J. E. Wiik, and J. Lemen, Hot and cool post-flare loops: Formation and dynamics, in *Magnetodynamic Phenomena in the Solar Atmosphere*, edited by Y. Uchida, T. Kosugi, and H. S. Hudson, pp. 211-212, Kluwer Acad., Norwell, Mass , 1996.

Sen, H. K., and M. L. White, A physical mechanism for the production of solar flares, *Sol. Phys.*, *23*, 146-154, 1972.

Shafranov, V. D., Plasma equilibrium in a magnetic field, *Rev. Plasma Phys.*, *2*, 103-151, 1966.

Simnett, G. M , and R. A. Harrison, The onset of coronal mass ejections, *Sol Phys.*, *99*, 291-311, 1985.

Sturrock, P. A , Maximum energy of semi-infinite magnetic field configurations, *Astrophys. J.*, *380*, 655-659, 1991.

Sturrock, P. A., P. Kaufmann, R. L. Moore, and D. F. Smith, Energy release in solar flares, *Sol. Phys*, *94*, 341-357, 1984.

Švestka, Z., *Solar Flares*, D. Reidel, Norwell, Mass., 1976.

Švestka, Z., Speeds of rising post-flare structures, *Sol. Phys.*, *169*, 403-413, 1996

Švestka, Z., and P. Simon, Proton flare project, 1966, *Sol. Phys.*, *10*, 3-59, 1969.

Švestka, Z., F. Farnik, P. Hick, H. S. Hudson, and Y. Uchida, Large-scale active coronal phenomena in Yohkoh SXT images, III, Enhanced post-flare streamer, *Sol. Phys.*, *176*, 355-371, 1997.

Thom, R., *Stabilité Structurelle et Morphogénèse*, Benjamin, White Plains, N. Y , 1972.

Titov, V. S., and P. Démoulin, Basic topology of twisted magnetic configurations in solar flares, *Astron Astrophys.*, *351*, 701-720, 1999.

Uchida, Y , Diagnosis of coronal magnetic structure by flare-associated hydromagnetic disturbances, *Publ. Astron. Soc. Jpn.*, *22*, 341-364, 1970.

Uchida, Y., Behavior of the flare produced coronal MHD wavefront and the occurrence of type II radio bursts, *Sol. Phys.*, *39*, 431-449, 1974.

van Ballegooijen, A. A., and P. C. H. Martens, Formation and eruption of solar prominences, *Astrophys. J.*, *343*, 971-984, 1989.

Van Tend, W., and M. Kuperus, The development of coronal electric current systems in active regions and their relation to filaments and flares, *Sol. Phys.*, *59*, 115-127, 1978.

Wagner, W. J., E. Hildner, L. L. House, C. Sawyer, K. V. Sheridan, and G. A. Dulk, Radio and visible light observations of matter ejected from the sun, *Astrophys. J.*, *244*, L123-L126, 1981.

Webb, D. F., C.-C. Cheng, G. A. Dulk, S. J. Edberg, S. F. Martin, S. L. McKenna, and D. J. McLean, Mechanical energy output of the 5 September 1973 flare, in *Solar Flares: A Monogram From the Skylab Solar Workshop*, edited by P. A. Sturrock, pp. 471-499, Colo. Assoc. Univ. Press, Boulder, Colo., 1980.

Webb, D. F., T. G. Forbes, H. Aurass, J. Chen, P. Martens, B. Rompolt, V. Rusin, S. F. Martin, and V. Gaizauskas, Material ejection: Report of the Flares 22 Workshop held at Ottawa, Canada May 1993, *Sol. Phys.*, *153*, 73-89, 1994.

Wolfson, R., Energy requirements for opening the solar corona, *Astrophys. J.*, *419*, 382-387, 1993.

Wolfson, R., and B. Dlamini, Cross-field currents: An energy source for coronal mass ejections?, *Astrophys. J.*, *483*, 961-971, 1997.

Wolfson, R., and B. C. Low, Energy buildup in sheared force-free magnetic fields, *Astrophys. J.*, *391*, 353-358, 1992.

Wolfson, R., and S. Saran, Energetics of coronal mass ejections: Role of the streamer cavity, *Astrophys. J.*, *499*, 496-503, 1998.

Yeh, T., Diamagnetic force on a flux tube, *Astrophys. J.*, *264*, 630-634, 1983.

Zirin, H., *Astrophysics of the Sun*, Cambridge Univ. Press, New York, 1988.

Zirin, H., and D. R. Lackner, The solar flares of August 28 and 30, 1966, *Sol. Phys.*, *6*, 86-103, 1969.

T. G. Forbes, Institute for the Study of Earth, Oceans, and Space, 39 College Road, University of New Hampshire, Durham, NH 03824. (terry.forbes@unh.edu)

(Received January 5, 2000; revised March 13, 2000;
accepted March 13, 2000.)